African Journal of Applied Research
Vol. 8, No. 2 (2022), pp. 332-343
http://www.ajaronline.com
http://doi.org/10.26437/ajar.31.10.2022.23

CONCEPT OF EQUIVALENT STRESS CRITERION FOR PREDICTING FAILURE OF BRITTLE MATERIALS

Sackey, S. M.[1] and Ngewana, T. Z.[2]
[1] *Department of Mechanical Engineering, Kwame Nkrumah University of Science and Technology, Ghana.*
[2] *Department of Mechanical Engineering, Cape Peninsula University of Technology, South Africa.*
sackeysm@yahoo.com

ABSTRACT

Purpose: A paucity of proven failure criteria for brittle engineering materials exists, and this paper intends to present and validate a novel concept of *equivalent stress criterion* for predicting the failure of brittle isotropic homogeneous materials based on the concept of effective causative failure stress.

Design/Methodology/Approach: Mathematical modelling is first performed based on strain-state equivalence, followed by conversion to the equivalent causative stress. The model is then validated with experimental and other data and with comparisons to traditional models. The material studied is BS 1452 Grade 250 continuous-cast grey cast iron with a Young's Modulus of 39 000 MPa and ultimate tensile strength of 290 MPa. The test samples were prepared square in shape 12 mm x 12 mm to enable stresses in two perpendicular directions. Data is generated from uniaxial and bi-axial tests, performed using a standard universal testing machine, INSTRON 880, improvised to enable bi-axial recordings.

Findings: Results point consistently to higher fidelity and transparency of the new model in representing the state of stress, especially in the second and fourth quadrants of the principal stress diagram, where Rankine's criterion completely ignores stress differences and Mohr handles shear stresses in a suboptimal fashion. Both the maximum principal stresses and maximum shear stresses predicted by the proposed model are found to be somewhat greater than those from the traditional models, indicating higher accuracy and greater aggressiveness in prediction. The findings have further revealed that shearing effects play a greater role in the failure of engineering brittle materials than traditional failure theories have considered.

Research Limitation: The study involved improvisation to enable biaxial stress recordings. This process was not perfect, resulting in smaller-than-ideal values of the lateral stresses.

Practical implication: The study recommended process and equipment development toward perfecting multiaxial tests.

Social implication: The survey will enrich the literature with pertinent design methodology to help in product design, including social-interest products.

Originality / Value: Since truly homogeneous materials are known to withstand very high hydrostatic pressures, direct stresses alone do not constitute valid failure criteria for all loading conditions.

Keywords: *Brittle. failure. modelling. shearing. stress.*
ISSN: 2408-7920

Arca Academic Publisher

African Journal of Applied Research
Vol. 8, No. 2 (2022), pp. 332-343
http://www.ajaronline.com
http://doi.org/10.26437/ajar.31.10.2022.23

INTRODUCTION

Material failure modelling and testing have been active areas of study for a great many years. The purpose of this paper is to present a novel concept of equivalent causative stress theory for predicting the failure of primarily brittle materials.

A long-standing failure theory for brittle materials, Mohr's criterion, suffers from a lack of mathematical rigour due to simplifying assumptions in its derivation, suboptimal treatment of shear stresses, and at times a lack of transparency regarding the mode of failure. Further back still, in time, Saint Venant's theory (*maximum-normal-strain* criterion), predicted the yielding failure of a specimen subjected to any combination of loads when the maximum normal strain at any point in the specimen reached the failure strain at the proportional limit (Karp & Durban, 2011; He, Ma, Karp, & Li, 2014). It was widely recognized and applied to engineering practice for many decades (He et al, 2014). The theory had the advantage that strains are often easier to measure than stresses Despite this, it became defunct due to its failure to account for hydrostatic effects and shear-stress effects (Wei, Zistl, Gerke, & Brünig, 2022).

In the modern era, there have been many attempts to develop criteria that apply to both ductile and brittle materials. These works include: a two-parameter yield criterion in principal stress space by Yu and Wang (2019), a strain-energy-based criterion by Lazzarin, Campagnolo, and Berto (2014) that averages energy over a material-dependent control volume; paraboloid and polynomial-invariant criteria distinguishing hydrostatic tension and compression effects (Gu & Chen (2018a, 2018b); unified criteria involving convex and other failure surfaces by Giraldo-Londoño and Paulino (2020); Qu et. al (2016); a general framework for ductile failure prediction based on size effects by Zheng et al (2022); a nonlinear generalized criterion based on fracture mechanics (Wang et al., 2022; Zuo et al., 2021); a failure initiation criterion for brittle materials with sharp notches (Yosibash et. Al., 2016a, 2016b); predictions of failure load and failure initiation angle to predict failure loads in steel structures by Yosibash et. al (2022); *failure* of pre-cracked brittle *materials* based on strain gradient elasticity by Vasiliev et. al (2021); analysis of elastic properties of brittle materials via indentation methods by Wu et. al (2019); a unified finite strain continuum approach for Modelling failure of quasi-brittle materials by Sun et al (2022) and a 3-D failure initiation criterion for a V-notched elastic brittle structures by Neuner et al (2022). Yu (2019) developed a theory based on the invariant *M*-integral to predict the structural integrity of damaged materials containing locally distributed defects. Pijak (2022) evolved a universal failure criterion for isotropic materials using energy formalism and polynomial invariants expansion while Pereira et al (2018) estimated the properties of isotropic materials as a basis for comparing numerical and experimental results.

This paper develops a theory to predict the failure of brittle isotropic engineering materials, attempting to address problems with traditional failure criteria. In the overall approach, a representation of *equivalent causative stress* is first developed and compared with the traditional models using both experimental and standard data.

ISSN: 2408-7920

African Journal of Applied Research
Vol. 8, No. 2 (2022), pp. 332-343
http://www.ajaronline.com
http://doi.org/10.26437/ajar.31.10.2022.23

METHODOLOGY

Initial Modelling

The aim of this section is to resolve the failure problem into a physically meaningful mathematical form that is objective and robust enough to be applicable to all cases.

In dealing with the age-long yet inconclusive debate over whether failure criteria should be formulated in terms of stresses or strain, the major argument in favour of stress says that specifying failure in terms of strains is inappropriate and internally inconsistent since it offers no compatibility with fracture mechanics in the brittle range and with dislocation mechanics in the ductile range. Furthermore, force (stress) is the overwhelmingly preferred form for molecular dynamics simulations. The counterargument says that since strains are a result of stresses, direct or indirect, it is the extent of strain in the material that eventually triggers its failure, and therefore any failure modelling must take this into account. Despite these well-grounded reasons in favour of either approach, the authors attempt to gain the best of both worlds by using both parameters, starting first with strain and then converting to stress.

In the main research approach, strain-state equivalence in the complex material is first established mathematically, followed by extraction of the *equivalent causative stress*, which is the single equivalent uniaxial direct stress that produces the same strain at failure as in uniaxial loading. Next, the equivalent maximum shear stress is determined from the equivalent causative stresses. This procedure can be shown to be more accurate than simply equating the maximum principal stress to its value in simple tension, as is done in the Rankine approach. In determining the equivalent causative stress, de-superposition of the principal stresses is employed (Figure 2).

Materials and data generation

Data for model validation is generated from uniaxial and ingenious bi-axial tests, performed using a standard universal testing machine (INSTRON 8801) improvised to enable bi-axial recordings. Uniaxial tests are natural to the machine and thus easy to perform. The material studied is BS 1452 Grade 250 continuous-cast grey cast iron with the following properties from the supplier: E = 39 000 MPa and σ_{UT} = 290 MPa, where E is Young's Modulus, and σ_{UT} is ultimate tensile strength. Outputs from the lab experiments include Young's Modulus, ultimate tensile strength, maximum load, tensile strain at rupture, and shear strength. The biaxial tests required improvisation to adapt the machine by measuring strains in the second (lateral) dimension with strain gauges and then calculating the stress from $\sigma = E\varepsilon$ using the average value of Young's Modulus outputted by the machine during the strength determinations. The test samples were prepared square in shape 12 mm x 12 mm so that the forces applied in two perpendicular directions easily constituted the principal stresses σ_1 and σ_2.

Validation

ISSN: 2408-7920

African Journal of Applied Research
Vol. 8, No. 2 (2022), pp. 332-343
http://www.ajaronline.com
http://doi.org/10.26437/ajar.31.10.2022.23

Model validation is done using both experimental data and comparisons with the traditional models. Further validation is performed using published standard material data for comparisons between the improved model and traditional theories.

MODELLING, RESULTS, AND VALIDATION

Modelling

Considering the biaxial load regime shown on the extreme left-hand side in Figure 1, strain equivalence in the *x*- or horizontal direction requires that

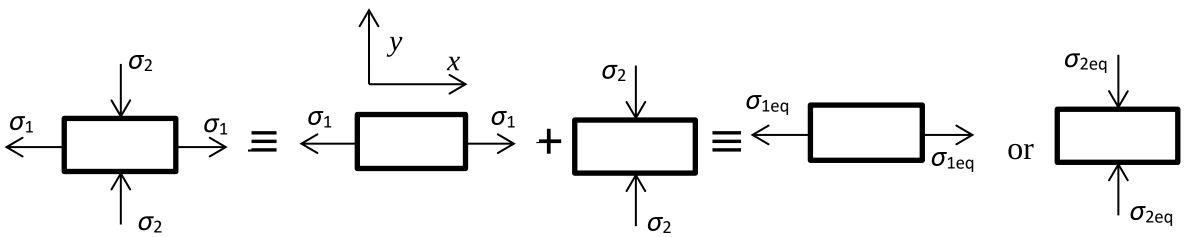

Figure 1. De-superposition (separation) of stresses to determine "equivalent" stress

$$\varepsilon_{xactual} = \varepsilon_{x1} + \varepsilon_{x2} = \frac{\sigma_1}{E} + \frac{\upsilon\sigma_2}{E} = \frac{\sigma_{1eq}}{E} = \varepsilon_{1eq} \quad (1)$$

where, clearly, the stress σ_{xeq} is equal to $\sigma_1 + \upsilon\sigma_2$, and where ε_{x1} and ε_{x2} are the strains in the *x*-direction due to principal stresses 1 and 2 respectively, and υ is the Poisson's ratio for the material under investigation.

A similar expression for the *y*- or vertical direction may likewise be written as

$$\varepsilon_{y1} + \varepsilon_{y2} = \frac{\sigma_2}{E} + \frac{\upsilon\sigma_1}{E} = \frac{\sigma_{2eq}}{E} = \varepsilon_{2eq} \quad (2)$$

Expressions for two other biaxial stress-state loading regimes, along with the above result, are displayed in Table 1.

The easy observation is that when the stresses are of opposite signs, the strains reinforce each other, thereby reducing load-carrying capacity, whereas if they are of like signs, the opposite effect occurs. Thus failure (brittle or yielding) by direct stress would occur under any state of stress if either the maximum normal strain corresponding to the greater of σ_{1eq} and σ_{2eq} reaches the critical value obtained from simple tests, or the maximum shear stress (Equation 3), reaches the limiting value, i.e., the strength of the material according to:

$$\tau_{\text{eqmax}} = \left(\frac{\sigma_{\text{1eq}} - \sigma_{\text{2eq}}}{2}\right) \quad (3)$$

ISSN: 2408-7920

The proposed *equivalent-causative-stress* criterion is now formally stated as follows:

> *Failure of a structural member under complex stresses occurs when the equivalent causative direct stress or the maximum equivalent shear stress exceeds the strength of the material.*

Expressed mathematically, failure of a part under complex stresses occurs when:

$$\sigma_{1eq} \geq \sigma_{UT}, \sigma_{UC} \qquad (4) \quad \text{or}$$

$$\sigma_{2eq} \geq \sigma_{UT}, \sigma_{UC} \qquad (5) \quad \text{or}$$

$$\tau_{\mathrm{eqmax}} \geq \tau_{\mathrm{U}}, \qquad (6)$$

whichever occurs first, i.e., whichever of (4) or (5) or (6) specifies a limiting failure stress value first is the one that determines the failure behaviour of the component under investigation. In the above equations, σ_{UT}, σ_{UC}, and τ_{U} are the failure stresses in tension, compression, and shear, respectively for the material. In the Rankine methodology, the greater of σ_1 and σ_2 simply would have been used instead, while with Mohr's approach the shear aspects are not adequately addressed.

Table 1 Equivalent stresses for three different stress-states

Stress-state	Equivalent Principal Stresses	Remarks
Biaxial tension-compression 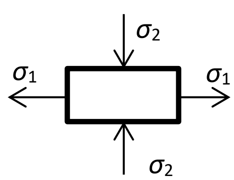	$\sigma_{1eq} = \sigma_1 + \upsilon\lvert\sigma_2\rvert$ $\sigma_{2eq} = -\lvert\sigma_2\rvert - \upsilon\sigma_1$	$\sigma_{1\mathrm{eq}}$ is greater than σ_1: load-carrying capacity reduces
Biaxial tension 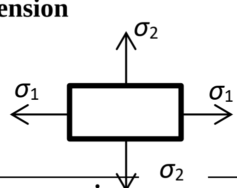	$\sigma_{1eq} = \sigma_1 - \upsilon\sigma_2$ $\sigma_{2eq} = \sigma_2 - \upsilon\sigma_1$	All stresses are positive $\sigma_{1\mathrm{eq}}$ is smaller than σ_1: load-carrying capacity increases
Biaxial compression 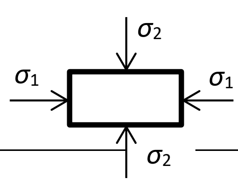	$\sigma_{1eq} = -\lvert\sigma_1\rvert + \upsilon\lvert\sigma_2\rvert$ $\sigma_{2eq} = -\lvert\sigma_2\rvert + \upsilon\lvert\sigma_1\rvert$	All stresses are negative $\sigma_{1\mathrm{eq}}$ is smaller than σ_1: load-carrying capacity increases

It may be observed from Table 1 that whenever the principal stresses are of the same sign (rows 2 and 3) hydrostatic effects come into play. It may thus be insightful to investigate the stiffness behaviour of the material under different stress states, including hydrostatic pressure.
Then, for the biaxial compression case, the net lateral strain in the *y*- and *x*-directions are:

ISSN: 2408-7920

African Journal of Applied Research
Vol. 8, No. 2 (2022), pp. 332-343
http://www.ajaronline.com
http://doi.org/10.26437/ajar.31.10.2022.23

$$\varepsilon_2 = -(\sigma_2 - \upsilon\sigma_1)/E = -(k - \upsilon)\, \sigma_1/E \qquad (7a)$$

$$\varepsilon_1 = -(\sigma_1 - \upsilon\, \sigma_2)/E \qquad (7b)$$

where $k = \sigma_2/\sigma_1$. Combining Equations (7a) and (7b), we get:

$$\varepsilon_2 = -(\sigma_2/E)\,(1 - \upsilon^2 - \upsilon\varepsilon_1 E/\sigma_2) \qquad (7c)$$

But $\varepsilon_1 E/\sigma_2 = -E(\sigma_1 - \upsilon\,\sigma_2)/\sigma_2 E = -(\sigma_1/\sigma_2 - \upsilon) = (k - \upsilon)$

Therefore, Equation (7c) becomes:

$$\varepsilon_2 = -(\sigma_2/E)\,(1 - \upsilon^2 - \upsilon(k - \upsilon)) \qquad (8)$$

The effective Young's modulus thus increases to:

$$E' = E/[1 - \upsilon^2 - \upsilon(k - \upsilon)] = E/(1 - \upsilon k) \qquad (8b)$$

In the above equations, k varies between 0 and 1. For $\sigma_2 > \sigma_1$ the positions of σ_2 and σ_1 are reversed in order not to violate this rule. It should be noted for example, that for a biaxial state of stress, $\sigma_2 = 0.5\sigma_1$ is equivalent to $\sigma_1 = 0.5\sigma_2$ in terms of the actual stress conditions created in a homogenous isotropic material, and therefore k must be 0.5 in each case.

For immovable lateral restraints, the strain ε_2 in that direction disappears giving, from (7a),

$$0 = -(k - \upsilon)\,\sigma_1/E \qquad \text{or} \qquad k = \sigma_2/\sigma_1 = \upsilon$$

This reduces Equation (8a) to

$$E' = E/(1 - \upsilon^2) = 1.1E\,, \qquad (9)$$

if υ is taken typically as 0.3, for illustration.

For the case where $k = 1$, so that $\sigma_1 = \sigma_2$, we get the equibiaxial loading condition which, from Equation (8a), yields

$$E' = E/(1 - \upsilon) = 1.43E \qquad (10)$$

again with $\upsilon = 0.3$.

The result represented by Equation (9) is already well-known. It is easily verified that when k takes on the values: $k = 0$, 0.3 (=υ, say), 0.5, and 1, then E' correspondingly varies as: E' = 1.0E, 1.1E, 1.2E, and 1.43E respectively. These hydrostatic effects can be compensated for in traditional failure theories, at least in part, provided the above adjustments in material stiffness can be made; something that most at best failure theories until now have neglected to do.

Results and Validation

The proposed model is now validated on the basis of both experimental data (Tables 2 and 3) and standard material data (Tables 4 and 5). Table 2 presents a summary of the data for the indicated material. Excluding outlier specimens 1 and 8, the key parameters are determined as:

$$E = 40\,000 \text{ MPa}$$
$$\sigma_{UT} = 300 \text{ MPa}$$

ISSN: 2408-7920

African Journal of Applied Research
Vol. 8, No. 2 (2022), pp. 332-343
http://www.ajaronline.com
http://doi.org/10.26437/ajar.31.10.2022.23

$$\varepsilon = 1.8\%$$
$$\tau_U = 320 \text{ MPa}$$

These values are in agreement with the material data from the supplier:

$$E = 39\ 000 \text{ MPa}$$
$$\sigma_{UT} = 290 \text{ MPa (250 MPa minimum)}$$

Table 2 Experimentally determined properties of BS 1452 Grade 250 Grey Cast Iron

Specimen	Tensile stress at Maximum Load (MPa)	Tensile strain (extension) Break (%)	Modulus, *E* (MPa)
1	230.661	0.6	57139
2	318.341	0.9	60178
3	328.026	1.5	39256
4	312.950	1.1	45216
5	311.093	1.2	43908
6	286.385	1.8	43398
7	316.341	1.4	40953
8	219.171	2.5	29110
9	288.266	2.3	12742
10	296.590	1.1	37209
11	199.016	1.3	60776
Mean	282.440	1.4	42717
Standard deviation	44.902	0.6	14057.756

Table 3 lays out data for the biaxial cases, while Figures 2 and 3 display graphically an example each of loading in the uniaxial and biaxial regimes.

Table 3: Biaxial loading cases (with exception of row 1)

Case	**Specimen**	**Strain ε_2**	**Stress σ_2 (MPa)**	**Stress σ_1 (MPa)**
1	3	0	0	328
2	7	10×10^{-6}	0.43	316
3	8	420×10^{-6}	16.8	219
4	9	170×10^{-6}	7.3	288
5	10	330×10^{-6}	14.1	297

Data source: Experimental tests (Biaxial)

ISSN: 2408-7920

African Journal of Applied Research
Vol. 8, No. 2 (2022), pp. 332-343
http://www.ajaronline.com
http://doi.org/10.26437/ajar.31.10.2022.23

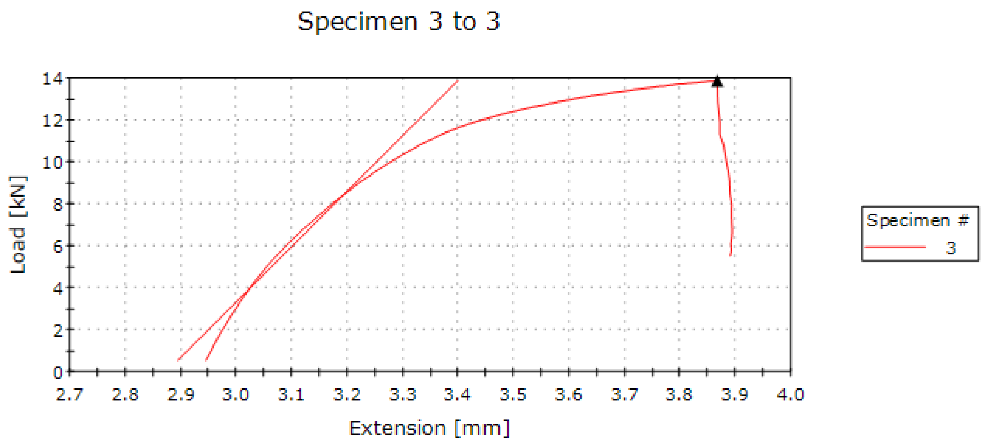

Figure 2: Uniaxial loading results (Specimen 4)

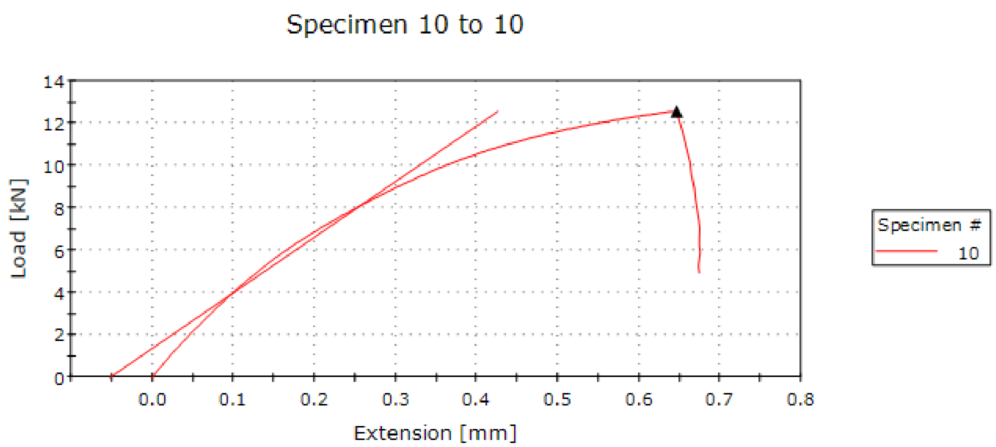

Figure 3: Biaxial tension–compression loading results (Specimen 10)

Other results involving both experimental and published standard material are laid out in Tables 4 and 5. In both tables column 4 determines whether the failure is predicted by any of the failure criteria by comparing the maximum stress (shear: τ_{max} or τ_{eqmax} or direct: σ_1, σ_2 or σ_{eq1}, σ_{eq2}) determined by calculation from each failure prediction model with the material's own strengths.

ISSN: 2408-7920

Table 4: Validation based on experimental data: brittle materials

Case 1 / **Criterion**	$\tau_{max} = R$ **(MPa)**	**Effective principal stress (MPa)**		**Failure Predicted? Y/N**	**Remarks**
	BS 1452 Grade 250 continuous-cast Grey Cast Iron $\upsilon = 0.21$ τ_U = 330 MPa σ_{UT} = 300 MPa, σ_{UC} = -660 MPa (estimated)				
Mohr	$\tau_{max} = 200$	$\sigma_1 = 100$	$\sigma_2 = -300$	N	Lacks clarity; for full evaluation τ_U needed
Rankine	$\tau_{max} = 200$	$\sigma_1 = 100$	$\sigma_2 = -300$	Y $\lvert\sigma_2\rvert > \sigma_{UT}$	Wrong prediction. σ_{UC} not considered
Proposed model	$\tau_{eqmax} = 234$	$\sigma_{1eq} = 151$	$\sigma_2 = -317$	N $\sigma_{1eq}<\sigma_{UT}$, $\sigma_{2eq}<\sigma_{UC}$	But τ_U needed for full evaluation

Table 5: Validation based on published standard data: brittle materials

Case 2 / **Criterion**	$\tau_{max} = R$ **(MPa)**	**Effective principal stress (MPa)**		**Failure Predicted? Y/N**	**Remarks**
	Cast Aluminium $\upsilon = 0.32$ $\tau_{U = N/A}$ σ_{UT} = 80 MPa σ_{UC} = -200 MPa				
Mohr	$\tau_{max} = 72.1$	$\sigma_1 = 32$	$\sigma_{2M} = -112$	N	Lacks clarity; for full evaluation τ_U needed
Rankine	$\tau_{max} = 72.1$	$\sigma_1 = 32$	$\sigma_{2R} = -112$	Y $\lvert\sigma_2\rvert > \sigma_{UT}$	Wrong prediction. σ_{UC} not considered
Proposed model	$\tau_{eqmax} = 95.2$	$\sigma_{1eq} = 69$	$\sigma_{2eq} = -122$	N $\sigma_{1eq}<\sigma_{UT}$, $\sigma_{2eq}<\sigma_{UC}$	But τ_U needed for full evaluation
Case 3	**Cast Aluminium** $\upsilon = 0.32$ $\tau_{U = N/A}$ σ_{UT} = 80 MPa σ_{UC} = -200 MPa				
Mohr	$\tau_{max} = 53.2$	$\sigma_1 = 68$	$\sigma_2 = -38$	Y	Lacks clarity τ_U rqd. for full evaluation
Rankine	$\tau_{max} = 53.2$	$\sigma_1 = 68$	$\sigma_2 = -38$	N $\sigma_1 < \sigma_{UT}$, $\sigma_2 < \sigma_{UC}$	τ_U rqd. for full evaluation
Proposed model	$\tau_{eqmax} = 70.2$	$\sigma_{1eq} = 80.4$	$\sigma_{2eq} = -59.96$	Y $\sigma_{1eq} > \sigma_{UT}$	Tensile failure, but τ_U required for check
Case 4	**Grey Cast Iron** $\upsilon = 0.2$ τ_U = 240 **MPa** σ_{UT} = 170 **MPa**, σ_{UC} = -655 **MPa**				
Mohr	$\tau_{max} = 200$	$\sigma_1 = 100$	$\sigma_2 = -300$	Y	Failure mode and reason not clear.
Rankine	$\tau_{max} = 200$	$\sigma_1 = 100$	$\sigma_2 = -300$	Y $\lvert\sigma_2\rvert > \sigma_{UT}$	Wrong prediction. σ_{UC} not considered
Proposed model	$\tau_{eqmax} = 234$	$\sigma_{1eq} = 151$	$\sigma_{2eq} = -317$	N $\sigma_{1eq}<\sigma_{UT}$, $\tau_{eqmax}< \tau_U$	More realistic. Offers clarity.

Material properties source for cases 2, 3, and 4: (Beer, 1992)

ISSN: 2408-7920

African Journal of Applied Research
Vol. 8, No. 2 (2022), pp. 332-343
http://www.ajaronline.com
http://doi.org/10.26437/ajar.31.10.2022.23

In these tables failure prediction by Mohr's criterion is done using the equations:

$$\sigma_{2M} = \left|\frac{\sigma_{UC}}{\sigma_{UT}}\right|\sigma_1 - |\sigma_{Uc}| \qquad (10) \qquad \text{Fourth quadrant,}$$

$$\sigma_{2M} = \left|\frac{\sigma_{UT}}{\sigma_{UC}}\right|\sigma_1 - |\sigma_{UT}| \qquad (11) \qquad \text{Second quadrant.}$$

Taking σ_1 as the independent variable we observe that a point in the second or fourth quadrant would fall outside Mohr's hexagon (indicating failure) if its value in absolute terms is greater than σ_2 in Equation (10) or (11).

DISCUSSION

From Tables 4 and 5, and Figures 2 and 3, it is clear that as the lateral compressive stress increases Young's modulus reduces, generally (a reverse of the hydrostatic case). This is one point where Saint Venant's theory failed, in not accounting for hydrostatic effects, which tend to strengthen the material to sustain higher loads than indicated by that theory (Wei, 2022; He, et al., 2014; Karp & Durban, 2011). In the actual experiments, it is observed that rupture in most of the biaxial cases occurred at the point of application of the lateral stress. This shows that compressive transverse stress reduces load-carrying capacity (He, et al., 2014). It has been shown that the stiffening effects can be accommodated by measured adjustments to the effective Young's modulus. The main advantage of the theory, that strains are often easier to measure than stresses, remains, though. Another inherent flaw of Saint Venant's criterion in that it ignores shear stress effects, as is somewhat the case with Mohr's criterion has been addressed by the new model.

For Case 2 (Table 5), Mohr's criterion and the proposed model both correctly predict no failure, unlike Rankine's. For case 3, even though the two criteria are again in agreement, this time they both predict failure while Rankine again predicts a contrary result; and whereas the proposed model reveals tensile action as the cause of this failure, with Mohr's criterion it is not so clear by what mode this predicted failure occurs. In all the above cases material strength evaluation is not complete until the shear strength of the material, τ_U, is also applied.

For case 4, Mohr's criterion and the proposed model are seen to be at variance concerning predicted values, but the former is in agreement with Rankine's. Once again Mohr's criterion fails to offer clarity regarding the cause of failure, whereas in the case of the proposed model the reasons for its prediction of no failure are obvious. As before, τ_U is required before full evaluation can be made.

Other attempts in the modern era to develop criteria that apply to brittle materials including a polynomial-invariant criterion distinguishing hydrostatic tension and compression effects by Gu and Chen (2018a, 2018b) are automatically covered by the rigour of the proposed theory.

ISSN: 2408-7920

Lastly, a recent attempt by Christensen (2016, 2018) to bridge the gap between failure criteria for isotropic homogeneous ductile and brittle materials warrants special comment in this context. In his work, Christensen developed a three-dimensional stress-based failure criterion built primarily on the von Mises criterion. For brittle materials, our analysis has shown that this criterion yields more conservative results for pure tensile stresses in the first and third quadrants of the principal stress diagram than both the Maximum Normal Stress and the Coulomb-Mohr criterion and thus could result in unnecessary overdesign as well as leave too large a room under mixed (tension and compression) loadings for error in its predictions.

CONCLUSION

It is unlikely that any major field falling under material applications research has had more effort expended with less to show for it than brittle materials failure modelling. Even the most prominent theories still need optimization. The primary aim of this paper has been to present and validate a criterion for predicting the failure of brittle materials based on the concept of effective causative failure stress to address problems with traditional failure criteria.

It has been shown that shearing effects play a greater role in the failure of brittle materials than traditional failure theories have considered, and this has been addressed in the proposed approach. The significance of this is that in evaluating a material's failure possibilities using non-energy methods, applied shear stresses and the material's shear strength must always be included in the analysis. In addition, truly homogeneous materials are known to withstand very high hydrostatic pressures without failing, indicating that maximum direct stresses alone do not constitute valid failure criteria for all loading conditions.

ACKNOWLEDGMENT

Acknowledgement is to the Faculty of Engineering of the Cape Peninsula University of Technology, South Africa, for supporting this work.

REFERENCES

Barsanescu, P. D., & Comanici, A. M. (2017). von Mises hypothesis revised. *Acta Mechanica*, *228*(2), 433-446.

Christensen, R. M. (2016). Perspective on materials failure theory and applications. *Journal of Applied Mechanics*, *83*(11).

Christensen, R., Li, Z., & Gao, H. (2018). An evaluation of the failure modes transition and the Christensen ductile/brittle failure theory using molecular dynamics. *Proceedings of the Royal Society A*, *474*(2219), 20180361.

Giraldo-Londoño, O., & Paulino, G. H. (2020). A unified approach for topology optimization with local stress constraints considering various failure criteria: von Mises, Drucker–Prager, Tresca, Mohr–Coulomb, Bresler–Pister and Willam–Warnke. *Proceedings of the Royal Society A*, *476*(2238), 20190861.

Gu, J., & Chen, P. (2018). A failure criterion for homogeneous and isotropic materials

ISSN: 2408-7920

distinguishing the different effects of hydrostatic tension and compression. *European Journal of Mechanics-A/Solids*, *70*, 15-22.

Gu, J., & Chen, P. (2018). A failure criterion for isotropic materials based on Mohr's failure plane theory. *Mechanics Research Communications*, *87*, 1-6.

He, L., Ma, G. W., Karp, B., & Li, Q. M. (2014). Investigation of dynamic Saint-Venant's principle in a cylindrical waveguide–Analytical results. *International Journal of Impact Engineering*, *73*, 135-144.

Karp, B., & Durban, D. (2011). Saint-Venant's principle in dynamics of structures. *Applied mechanics reviews*, *64*(2).

Lazzarin, P., Campagnolo, A., & Berto, F. (2014). A comparison among some recent energy- and stress-based criteria for the fracture assessment of sharp V-notched components under Mode I loading. *Theoretical and Applied Fracture Mechanics*, *71*, 21-30.

Qu, R. T., Zhang, Z. J., Zhang, P., Liu, Z. Q., & Zhang, Z. F. (2016). Generalized energy failure criterion. *Scientific reports*, *6*(1), 1-8.

Sun, Y., & Xiang, Z. (2022). A semi-analytical quasi-brittle fracture criterion for elliptical notches. *Engineering Fracture Mechanics*, *266*, 108405.

Vasiliev, V., Lurie, S., & Solyaev, Y. (2021). New approach to failure of pre-cracked brittle materials based on regularized solutions of strain gradient elasticity. *Engineering Fracture Mechanics*, *258*, 108080.

Wang, Z., Pan, P., Zuo, J., & Gao, Y. (2022). A generalized nonlinear three-dimensional failure criterion based on fracture mechanics. *Journal of Rock Mechanics and Geotechnical Engineering*.

Wei, Z., Zistl, M., Gerke, S., & Brünig, M. (2022). Analysis of ductile damage and fracture under reverse loading. *International Journal of Mechanical Sciences*, *228*, 107476.

Wu, S.J., Chin P.C. & Liu H. (2019), Measurement of elastic properties of brittle materials by ultrasonic and indentation methods, *Appl Sci*, 9 (10) 2067.

Yosibash, Z., & Mittelman, B. (2016). A 3-D failure initiation criterion from a sharp V-notch edge in elastic brittle structures. *European Journal of Mechanics-A/Solids*, *60*, 70-94.

Yosibash, Z., Mendelovich, V., Gilad, I., & Bussiba, A. (2022). Can the finite fracture mechanics coupled criterion be applied to V-notch tips of a quasi-brittle steel alloy? *Engineering Fracture Mechanics*, *269*, 108513.

Yu, N. Y., Li, Q., & Chen, Y. H. (2013). Experimental evaluation of the M-integral in an elastic-plastic material containing multiple defects. *Journal of Applied Mechanics*, *80*(1).

Yu, L., & Wang, T. C. (2019). Generalized Mohr-Coulomb strain criterion for bulk metallic glasses under complex compressive loading. *Scientific Reports*, *9*(1), 1-9.

Zheng, L., Wang, K., Jiang, Y., Wan, M., & Meng, B. (2022). A new ductile failure criterion for micro/meso scale forming limit prediction of metal foils considering size effect and free surface roughening. *International Journal of Plasticity*, *157*, 103406.

Zuo, S., Hu, C., Zhao, L., Jiao, K., Lei, Z., Huang, D., & Zhu, Z. (2021). Reliability back analysis of a 3D wedge slope based on the nonlinear Barton-Bandis failure criterion. *Engineering Failure Analysis*, *128*, 105601.

ISSN: 2408-7920

Arca Academic Publisher